Volume 21
Number 46
14 December 2025
Pages 8763–8952

Soft Matter

rsc.li/soft-matter-journal

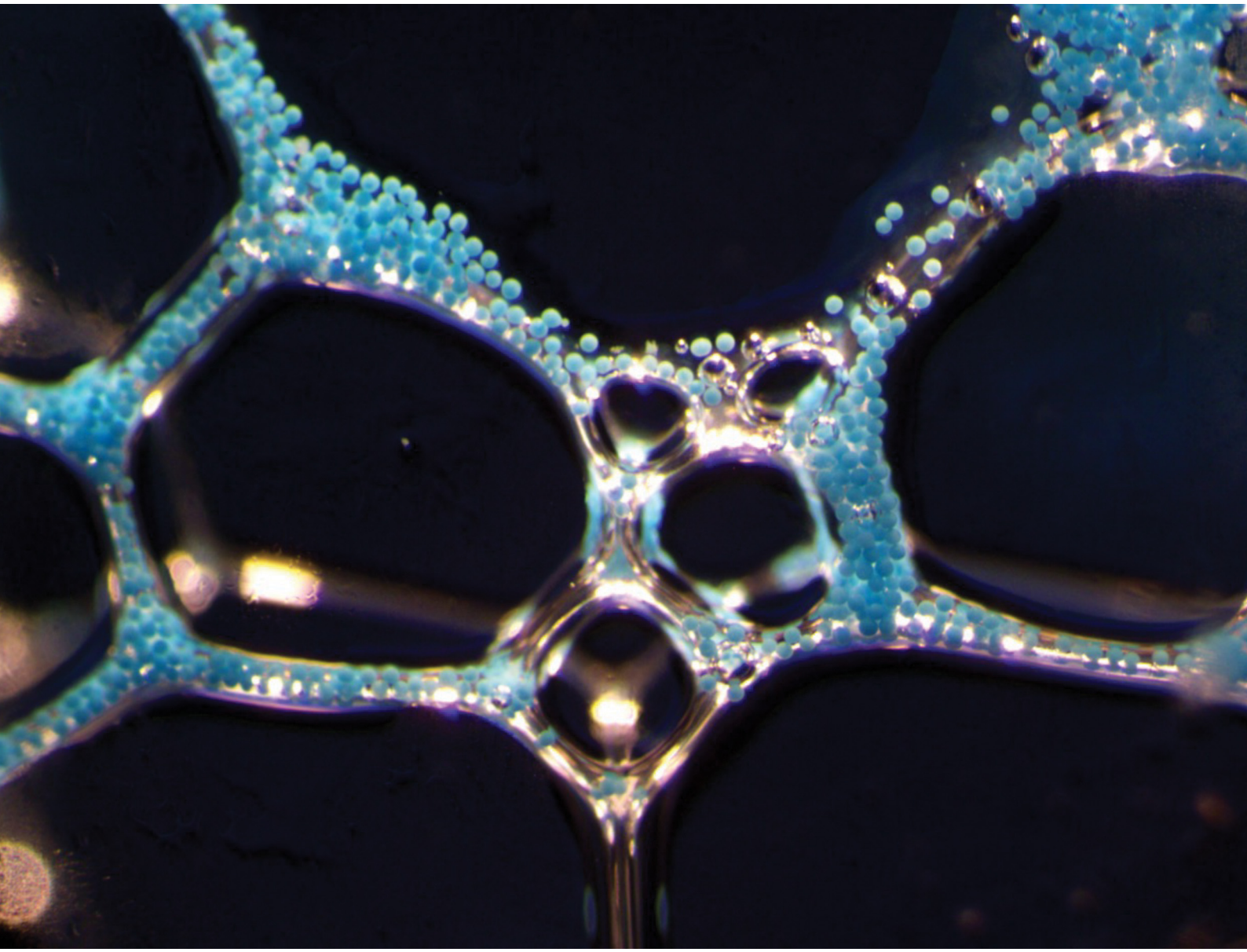

ISSN 1744-6848

ROYAL SOCIETY OF CHEMISTRY

PAPER
Bhuvnesh Bharti *et al.*
Fatty acid foams for nonselective physical removal of microplastics from aqueous solutions

20 YEARS ANNIVERSARY

Soft Matter

PAPER

View Article Online
View Journal | View Issue

Cite this: *Soft Matter*, 2025, **21**, 8771

Fatty acid foams for nonselective physical removal of microplastics from aqueous solutions

Kennedy A. Guillot,[a] Philip J. Brahana,[a] Joseph C. Romanos,[a] Gernot Rother,[b] Michael G. Benton[a] and Bhuvnesh Bharti *[a]

Received 22nd August 2025,
Accepted 15th October 2025

DOI: 10.1039/d5sm00850f

rsc.li/soft-matter-journal

Microplastics (MPs) are pervasive environmental contaminants whose removal from water remains a major challenge due to their small size, chemical diversity, and dynamic surface properties arising from environmental aging/weathering. Here, we present a concept of foam-based separation method that physically traps MPs in the foam phase using microtubular assemblies of 12-hydroxystearic acid. These foams are stabilized by anisotropic fatty acid microtubules formed in the presence of ethanolamine, which jam within the foam channels and suppress fluid drainage thereby enhancing MP retention and foam stability. MPs of different sizes, polymer compositions (including polystyrene, polypropylene, polyethylene terephthalate, and polytetrafluoroethylene), and weathered states were retained in the foam phase without requiring chemical modification or relying on chemical interactions between the fatty acid and MPs. Thermally induced transition of the fatty acid microtubules into nanomicelles above the characteristic phase transition temperature (~35 °C) enables controlled foam collapse and recovery of trapped MPs. The cumulative removal efficiency can exceed 85% through multiple foaming cycles, matching predictions from a probabilistic retention model. This work shows that foams can provide a simple platform to trap MPs, thus providing a new physical-removal strategy that does not rely on the particles' chemistry.

1. Introduction

Plastic pollution is one of the defining environmental issues of this century. The exponential rise in plastic manufacturing since the industrial revolution, coupled with improper disposal practices, has led to an unprecedented pollution crisis.[1] One specific class of plastic pollutants currently being extensively discussed are microplastics (MPs). MPs are plastic particles ranging in size from[2] 1 to 1000 μm. These micron-sized contaminants have been detected even in remote environments,[3–5] illustrating their highly dispersive transport properties[6] and persistence in natural environments. MPs enter the environment as either primary MPs, which are directly released during manufacturing or use, or secondary MPs, which result from the breakdown of larger plastic debris due to environmental stressors.[6] Regardless of entry pathway, MPs exhibit a higher surface-to-volume ratio relative to their macroscopic counterparts. This elevated surface-to-volume ratio amplifies the dominance of surface forces over bulk forces in governing their interactions and behavior.[6] The physicochemical properties of MPs are dynamic and often rapidly evolve in response to environmental stressors such as sunlight. These dynamically changing surface properties of MPs alter their behaviors, including transport properties, their capacity to adsorb coexisting pollutants,[7–10] and their ability to act as ice-nucleating particles.[11] While the immediate impacts of MPs on environmental health are still under investigation, there is a pressing need to reduce MP pollution and develop effective methods for their removal from the environment.

Micron-sized pollutant particles can be removed from water using methods such as coagulation, flocculation, filtration, and adsorption.[12,13] These techniques typically involve aggregating or trapping the particles for easier removal. Coagulation using molecular or ionic coagulants is a crucial step in water treatment to precipitate suspended particulate matter in flocs, which settle or are filtered out.[14] Another effective method is froth flotation. This process introduces air bubbles into the water to carry hydrophobic particles to the surface. Surfactants are added to alter the wettability of the particulates and enable their attachment to air bubbles, thus separating suspended mineral particles and other hydrophobic pollutants.[15,16] However, these traditional methods often rely on defined chemical compositions of the particulate matter. For instance, coagulation and flocculation depend on specific interactions between coagulants and the surface of the particles.[14] In the same way,

[a] *Cain Department of Chemical Engineering, Louisiana State University, Baron Rouge, LA 70803, USA. E-mail: bbharti@lsu.edu*
[b] *Neutron Scattering Division, Oak Ridge National Laboratory, Oak Ridge, TN 37830, USA*

effectiveness of froth flotation process can vary based on the hydrophobicity of the particles and their interaction with surfactants.[15] This reliance on surface chemistry can make it difficult to remove a wide variety of particulate pollutants with diverse surface chemistries, including MPs.

MPs do not always maintain the same surface properties as their parent plastics or when they were initially manufactured. Environmental aging processes, such as photooxidation[17] and biodegradation,[18,19] significantly alter the surface characteristics of MPs, making them hydrophilic and potentially less responsive to conventional water treatment approaches. In this article, we present a strategy to overcome these challenges by combining froth flotation with the physical entrapment of particulate matter in the foam phase using the microtubular self-assembled state of fatty acid molecules. We show that this fatty acid foam-based method does not significantly depend on the chemical composition of the MPs, providing a more versatile solution for MP removal from aqueous environments.

Fatty acid molecules consist of a hydrocarbon tail and a carboxylic acid headgroup. The interfacial behavior and self-assembly of these molecules in aqueous solutions depend on their chemical structure, solution pH, and the presence of counterions.[20–22] Among various fatty acids, 12-hydroxystearic acid (12-HSA) is widely used due to its benign chemical properties and the tunability of the self-assembled structures.[23] The pairing of 12-HSA with specific organic counterions can direct the formation of diverse assemblies, including ribbons, helices, tubules, or micelles. In this work, we leverage the self-assembly of 12-HSA into microtubular structures to produce ''ultra-stable'' foams that resist collapse by preventing fluid drainage at room temperature.[23,24] Upon foam formation, the anisotropic geometry of 12-HSA microtubules causes them to jam within the foam's thin liquid channels, significantly slowing or halting drainage of fluid from foam to bulk phase. We demonstrate that this jammed microstructure can efficiently trap and separate MPs. Furthermore, the well-established thermally induced transition of microtubules into nano-sized micelles offers a convenient, on-demand method to destabilize the foam, providing a practical route for isolating and recovering the captured MPs.[25]

In this article, we present a fatty acid-based, eco-friendly foam that utilizes 12-HSA microtubules to capture and remove MPs from water. Previous studies have explored pollutant removal using protein-based and Pickering foams stabilized by colloidal or biomolecular particles;[26,27] however, these approaches rely on specific stabilizing agents or surface chemistry of the particles. In contrast, the fatty acid-based foams presented here are stabilized solely by self-assembled microtubules of 12-HSA, offering a distinct route to generate stable foams capable of physically entrapping diverse MPs. Unlike conventional approaches, our method does not rely on specific particle surface chemistries for the MP removal process, making it broadly effective for MPs subjected to various environmental stressors. We quantify the MP retention efficiency of the foam across multiple types of common MPs, including polyethylene, polystyrene, polypropylene, and polytetrafluoroethylene, as well as MPs of different sizes and weathering stages. Therefore, physical entrapment of MP in foams could form a basis for new, more efficient MP removal methods.

2. Results and discussion

2.1. Model fatty acid, counterions, and microplastics

Fatty acids are excellent foaming agents due to their emulsifying and surface tension-reducing properties. We selected 12-HSA as a model fatty acid due to its three key attributes:[28] (1) environmentally benign nature; (2) ability to self-assemble into diverse supramolecular structures, such as nanomicelles and microtubules, depending on the choice of counterion; and (3) reversible transition between nanomicellar and microtubular states near 35 °C. The structural tunability of 12-HSA makes it a promising material for MP removal applications. We use small-angle X-ray scattering (SAXS) to characterize the self-assembled morphologies of 12-HSA (10 mg mL^{-1}, TCI, >75% purity) in aqueous solutions containing either ethanolamine (Sigma-Aldrich, >98% purity) or choline (Sigma-Aldrich, 46% in water) as counterions at fatty acid to counterion molar ratio (R) of 0.5. The SAXS measurements were carried out on the Xenocs Xeuss 3.0 SAXS/WAXS instrument at Oak Ridge National Laboratory. Samples were placed in 2 mm glass capillaries and measured for 30 minutes. Empty cell scattering was subtracted from sample scattering curves.

SAXS profiles of 12-HSA with ethanolamine show distinct Bragg peaks at momentum transfers $q \approx 0.02$ $Å^{-1}$ and 0.04 $Å^{-1}$ (Fig. 1a). The Bragg peaks are the signature of the ordered domains of 12-HSA with interlamellar spacing of 31.4 nm ($2\pi/q$) within the microtubule. This separation corresponds to one lipid bilayer plus one water layer, as reported previously.[29] The microtubules are also observed in the optical microscope image (Fig. 1a, inset), further confirming their formation using ethanolamine as the counterion. In contrast, no Bragg peaks were observed for 12-HSA solution prepared using choline as the counterion, suggesting the formation of nanomicelles which remain undetectable by optical microscopy (not shown). The formation of nanomicelles at room temperature with choline at R = 0.5 agrees with previous reports.[30]

The counterions partially immobilize near the deprotonated carboxylate headgroups of 12-HSA, thereby modulating intermolecular interactions and tuning the effective packing parameter that governs the resulting supramolecular structure.[31] Choline, with its large and sterically hindered quaternary ammonium structure, disrupts tight molecular packing of 12-HSA and promotes the formation of nanomicelles. In contrast, ethanolamine being smaller and less hindered facilitates the formation of extended bilayer structures of 12-HSA. These bilayers, organized with alternating layers of 12-HSA and aqueous counterions, undergo spontaneous twisting due to the chirality at the 12th carbon, ultimately yielding multilamellar microtubes.[32] These microtubules exhibit high aspect ratios and structural rigidity, which significantly enhance stability of foam formed by its solution. In the foam phase, the microtubules

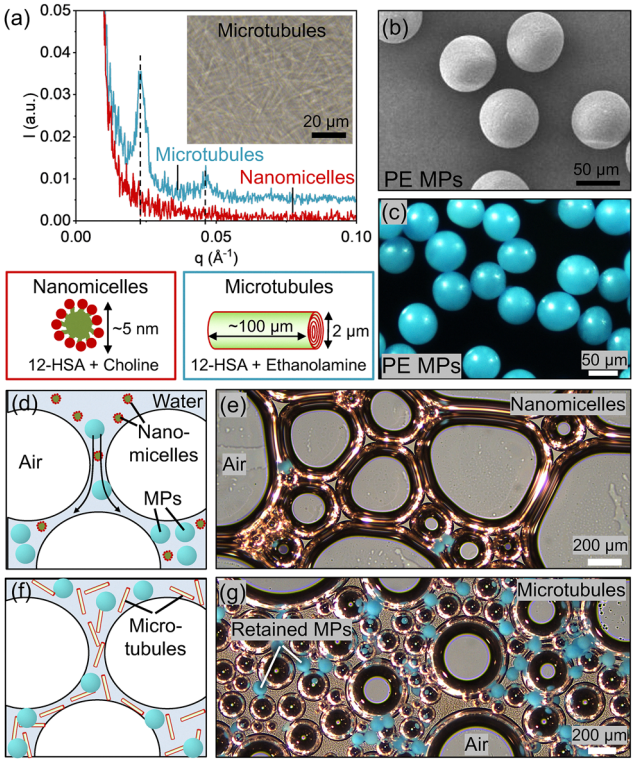

Fig. 1 (a) Small-angle X-ray scattering (SAXS) intensity profile for aqueous solution of 10 mg mL^{-1} 12-HSA with choline (red line) and ethanolamine (blue line) as counterions at fatty acid to counterion molar ratio R = 0.5 and 25 °C. The Bragg peaks at 0.02 Å^{-1} and 0.04 Å^{-1} for 12-HSA with ethanolamine are the signature of the multilamellar structure of the microtubules, which are absent for the nanomicelles formed with choline. The schematics of the nanomicelles and microtubule structures shown under the SAXS data are not drawn to scale. (b) and (c) Scanning electron micrograph (SEM) and optical microscope image of the polyethylene (PE) particles used as model MPs in the study. The model PE MPs were spherical in shape, nearly neutrally buoyant, and pre-dyed with blue color for improved visualization. (d)–(g) Schematic representation and optical microscope images of foams formed by 12-HSA in their (d) and (e) nanomicellar and (f) and (g) microtubular self-assembled states. (d) and (e) PE MPs drain out from the foam to bulk solution for 12-HSA in nanomicellar form at room temperature (choline as counterion). (f) and (g) Microtubular form of 12-HSA (ethanolamine as counterion) shows effective trapping of the MPs in the foam phase.

act as physical barriers to liquid drainage, thereby suppressing foam collapse.[21,33,34] We aim to leverage this stability mechanism of the 12-HSA foams to physically trap and retain MPs within the foam phase.

To systematically evaluate the effectiveness of 12-HSA based foams for MP removal, we first used polyethylene (PE) microspheres as a model system. PE was chosen due to its high environmental prevalence, accounting for approximately 11–32% (by number) of MPs reported in aquatic environments.[35] Commercially available spherical PE particles (Cospheric LLC) with an average diameter of ~65 μm were selected for these experiments (Fig. 1b, c, and Fig. S1). These particles were dyed blue to facilitate visual tracking and engineered to be nearly neutrally buoyant in water, with a mass density ~1.0 g cm^{-3}. The use of such well-characterized and uniform particles as model MPs enabled precise quantification of their removal efficiency using fatty acid foams. Beyond the PE microsphere model system, we also assessed the broader applicability of our foam-based separation strategy by testing MPs generated through mechanical abrasion of commonly used macroplastics with different chemistries, including polystyrene, polypropylene, polyethylene terephthalate, and polytetrafluoroethylene.

2.2. Microplastic retention in aqueous foams

The self-assembled state of fatty acids governs MP capture and retention in the foam phase. We compared MP retention in foam phase formed by the solutions of 10 mg mL^{-1} 12-HSA with either ethanolamine or choline as counterion at R = 0.5. This molar ratio was chosen based on previous findings demonstrating that 12-HSA with ethanolamine at R = 0.5 yields ultra-stable foams.[34] In our experiments, 1.5 mg of spherical PE MPs were introduced into 1 mL of a 10 mg mL^{-1} 12-HSA solution prepared using either choline or ethanolamine counterions. Subsequently, the foam was generated by vigorous shaking. Immediately after foam generation, MPs partitioned between the foam phase and the underlying bulk solution. The retention of MPs within the foam phase was enabled by the structural characteristics of the self-assembled state of 12-HSA in the thin liquid channels separating the foam bubbles. These self-assembled structures can increase foam stability and reduce liquid drainage kinetics, supporting MP retention within the foam. The distribution and partition of MPs among the foam and bulk phases were observed using optical imaging and quantified by subsequent image analysis using ImageJ (discussed below).[36]

In foams formed by 12-HSA with choline, MPs readily drain back into the bulk phase depleting the MPs in the foam phase. This was confirmed by microscope imaging, where no significant MPs were present in the foam channels (Fig. 1d and e). Conversely, the MPs were retained and trapped in the foam formed by 12-HSA with ethanolamine, where significant amounts of MPs (blue) appeared in the liquid channels between the bubbles (Fig. 1f and g). To quantify the degree of retention of MPs in the foam phase, we placed the vigorously shaken solution in a rectangular cuvette of dimensions 1 cm × 1 cm × 10 cm and monitored the change in the concentration of MPs in bulk phase over 280 minutes (Fig. 2a–c). We used ImageJ to determine the change in the number density of MP particles in the bulk solution with observation time (see SI). The MP retention efficiency of the foam is calculated as

$$\text{Retention efficiency, RE}(t) = \left(\frac{N_0 - N(t)}{N_0}\right) \times 100 \qquad (1)$$

where t is the time elapsed since shaking, N_0 and N respectively are the number density of MPs (per unit area) in the bulk solution prior to the foam formation and after time t of foam formation. The values of N_0 and N are measured in a 40 mm^2 area immediately below foam-bulk interface. Note that N is the function of t and directly quantifies the number of MPs drained or "re-entering" bulk solution from the foam phase. Hence the value of $N_0 - N(t)$ is the semi-quantitative measure of the MPs

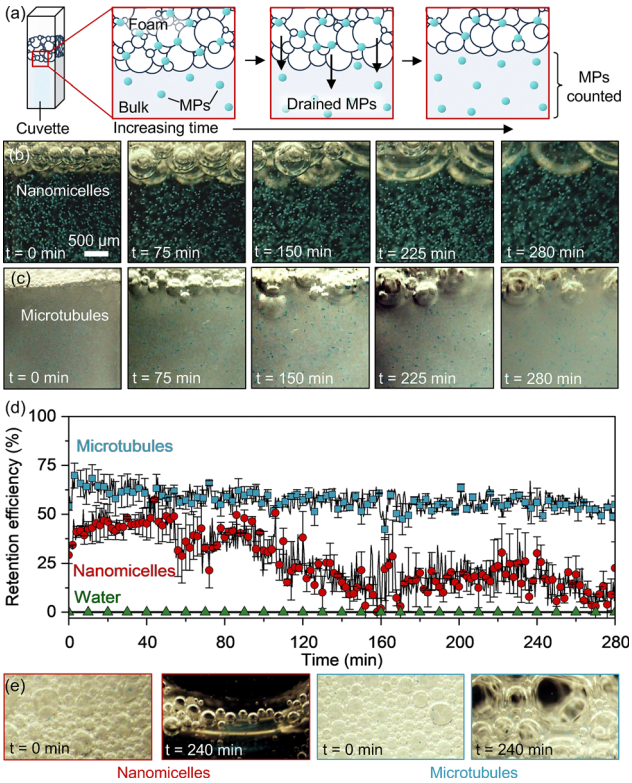

Fig. 2 (a) Schematic representing the experimental setup for semi-quantitative determination of the MP drainage to bulk and thus allowing the estimation of the MP retention efficiency of 12-HSA foam. (b) and (c) Image sequences taken near the foam-bulk solution interface for 12-HSA forming nanomicelles (b) and microtubules (c). The larger number density of MPs in the case of nanomicelle foam indicates the draining and re-entering of MPs into bulk phase from the foam, whereas the MPs remain trapped in the foam formed by 12-HSA microtubules. (d) The change in the MP retention efficiency of foam phase after the initial foam formation in the solutions containing only water *i.e.*, no 12-HSA (green triangles), nanomicelles (red circles) and microtubules (blue squares) of 12-HSA. The impact of gravity was minimized during experimentation using nearly neutrally buoyant MPs and additionally stirring the bulk solution at low rates (60 rpm) and thus preventing MPs from settling without significantly disrupting the foam. The error bars represent the standard error of three experiments. (e) Images of the foam-bulk interface at t = 0 minutes and 240 minutes for the foams formed by 12-HSA in its nanomicellar and microtubular states. The nanomicellar foam fully collapses after 240 minutes, which is not the case for foams formed by microtubules.

trapped in the foam phase and allows estimating MP retention efficiency of the foam.

The foams formed by 12-HSA in its microtubular state show efficient retention of MPs. The changes in the MP retention efficiency in the region below the foam-bulk solution interface for 12-HSA in nanomicellar and microtubular states is shown in Fig. 2d. We find that immediately after vigorous shaking of the solution, *i.e.*, t = 0 minutes, the MP retention efficiency of foams formed by microtubules is 60–70%, whereas for nanomicellar foam it is 40–50% (Fig. 2d). After t = 280 min, the MP retention capacity decreases to ~5% and ~55% respectively for nanomicellar and microtubular foams. The observed decline in MP retention efficiency with time reflects the gradual drainage of MPs from the foam into the bulk solution. The microtubular foam exhibits a slower and less pronounced decrease in MP retention efficiency compared to the nanomicelles. This behavior is attributed to higher degree of foam stability and the physical resistance to the fluid drainage from the narrow channels between the bubbles in the presence of microtubules in the foam. The small-sized nanomicelles formed by 12-HSA using choline as counterion do not provide any physical barrier against the draining fluid and subsequent thin-film collapse. Conversely, the 12-HSA with ethanolamine as counterion forms larger microtubules that create a more stable foam matrix.[34] These microtubules trap and retain MPs within the foam, limiting their mobility and preventing them from escaping into the bulk phase. Note that no foam is formed in the absence of 12-HSA, hence the MP retention efficiency for water remains 0% throughout the experimental period (Fig. 2d).

The above experiments show the proof-of-concept of using microtubule-stabilized foams to retain MPs in the foam phase, but two immediate and obvious issues with the method are: (1) mere partitioning of the MP into the foam phase and not removal; and (2) suboptimal MP retention with maximum MP retention efficiency of 50–60% (after 15 minutes). To address both these challenges, we use the thermoresponsive nature of the 12-HSA microtubules formed with ethanolamine, which allows separating and isolating MPs from the foam, as well as improving the MP removal *via* multi-cycle process (discussed below).

2.3. Isolating microplastics from foam and enhancing retention efficiency

The MPs can be effectively isolated by first separating the microtubular foam with trapped MPs from the bulk liquid and subsequently destabilizing the foam on demand *via* heating. The microtubules formed by 12-HSA using the ethanolamine counterion show thermoresponsive behavior, undergoing a reversible transition from the microtubular state at 25 °C to nanomicellar states above a characteristic phase transition temperature of ~35 °C, as confirmed by optical microscopy (Fig. 3a). This transition is driven by thermal disruption of hydrogen bonding and other non-covalent interactions stabilizing the microtubular state.[37,38] At elevated temperatures, nanomicelles represent a thermodynamically preferred state due to reduced anisotropic intermolecular forces. To highlight the utility of this thermally induced phase transition for MP separation, we first prepared a foam using a 10 mg mL^{-1} 12-HSA solution with ethanolamine at R = 0.5 and introduced PE MPs at a concentration of 1.5 mg mL^{-1}. After the MPs were retained in the microtubular foam phase, the foam was carefully separated and transferred into an empty rectangular quartz cuvette (Fig. 3b). To release the trapped MPs, the foam phase is destabilized by heating the cuvette to temperatures above 35 °C, which induces a microtubule-to-nanomicelle transition. Infrared imaging confirmed a gradual increase in temperature of the foam (Fig. 3c), which coincided with progressive foam collapse. This thermoresponsive behavior of the microtubules enhances MP removal efficiency and enables

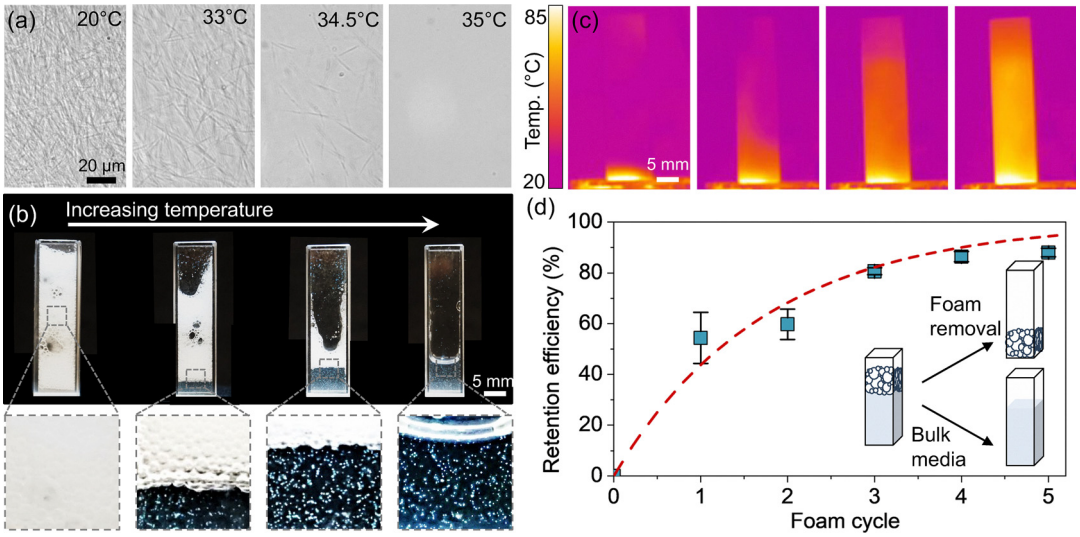

Fig. 3 (a) Optical microscope images showing the phase transition of 12-HSA microtubules to nanomicelles upon increasing the temperature of the solution above the critical value of 35 °C. (b) Images showing the foam phase with retained microplastics separated from the bulk solution, transferred to a cuvette and placed on a heating plate. The addition of heat induces the microtubule to nanomicelle transition, leading to foam deconstruction and thus releasing MPs in the liquid phase. The gradual release of MPs coinciding with this phase transition is shown in the insets below the corresponding cuvette. (c) Infrared images of the cuvette showing the gradual change in temperature across the cuvette, leading to the release of retained MPs. (d) The change in the MP retention efficiency of microtubular foam through multiple foam cycles. Here the foam was removed after 15 minutes of equilibration, and the remaining liquid bulk phase was again shaken vigorously to produce foam for the subsequent cycle. The MP retention efficiency reported here is the cumulative value of multiple foaming and separation cycles. The squares represent the experimental data, and the dashed line represents the cumulative retention efficiency predicted based on single-cycle retention probability.

isolation of the MPs by cycling the foams through microtubular and nanomicelle states corresponding to MP retention and release steps.

MP removal is further enhanced upon implementing a multi-cycle foaming process (Fig. 3d). The experimental setup followed the same protocol described above and was applied exclusively to the microtubular foams of 12-HSA, given its superior MP retention efficiency compared to the nanomicelles. Each foaming cycle consisted of three steps: (1) vigorous shaking to generate the foam from water; (2) allowing the foam to equilibrate for 15 minutes; and (3) isolating the foam and transferring it to a clean cuvette (Fig. 3d inset). Successive foam cycles progressively increased the cumulative MP removal from the bulk suspension (Fig. 3d). We observed that the total MP retention efficiency (cumulative) improved with each cycle, reaching a maximum of ~85%. This value is comparable to removal efficiencies reported in water treatment facilities employing methods such as coagulation or filtration.[39,40] Assuming the retention efficiency remains constant across cycles and using basic probability theory, the cumulative MP retention efficiency after n foaming cycles can be expressed as $RE_n = (RE_1)^n$, where RE_1 is the retention efficiency of a single cycle. This probabilistic model (dashed line in Fig. 3d) complements the experimental trend and could enable reasonable prediction of total MP removal over multiple foam cycles. Note that the assumption of constant single-cycle efficiency is a fundamental limitation of the model, which could vary cycle to cycle under practical conditions. Importantly, the MP removal mechanism using microtubular foams is primarily physical, rather than chemical. Hence, our approach will allow trapping MPs irrespective of their surface chemistry. To demonstrate the robustness of this mechanism, we evaluated MP retention efficiency of PE MPs of smaller size and dissimilar surface chemistry altered by the weathering/photooxidation of the MPs.

2.4. Effects of weathered state and size of microplastic

Current MP removal strategies often depend on particle surface chemistry, leveraging hydrophobicity, charge, or specific chemical affinities to achieve effective separation.[14–16,41] However, such approaches face limitations due to the dynamic and heterogeneous nature of MP surfaces in the environment. While most pristine plastics are inherently hydrophobic, prolonged exposure of MPs to sunlight and oxygen in the environment can lead to their photooxidation, introducing polar functional groups such as carboxyl on the surface.[42,43] This transformation due to environmental weathering increases the hydrophilicity of MPs and alter their surface interactions and adsorption behaviors.[7,17] To assess the robustness and surface chemistry independence of our microtubule foam-based MP removal method, we performed controlled photooxidation of polyethylene PE MPs followed by foam separation experiments at different weathering stages. Photooxidation is a dominant environmental aging mechanism for polyolefins such as PE and is known to increase surface wettability through oxidative modification.[17,42] To simulate this effect under controlled conditions, we subjected PE MPs artificial aging in a QUV chamber (Q-Lab Corp.) following ASTM standard D5071. In a typical experiment, 100 mg of MPs were dispersed over

the air–water interface of 100 mL deionized water in cleaned glass containers, forming a monolayer configuration. These containers were then exposed to UV light generated from a xenon arc lamp with an irradiance of 0.35 W m^{-2}. Before encountering the MPs, the UV light passes through a 340 nm wavelength filter, which yields conditions comparable to natural sunlight. The artificial aging chamber temperature was maintained at 63 °C *via* air cooling to accelerate and simulate the environmental photooxidation process.[44] Note that in this article we refer to the artificial aging and accelerated weathering synonymously, where one day in the weathering chamber corresponds to approximately 10–30 days of outdoor exposure, depending on environmental conditions and geographic location.[17]

To confirm the extent of surface chemical modification *i.e.*, photooxidation induced by accelerated weathering, we characterized the MPs using X-ray photoelectron spectroscopy (XPS). As early as two days of accelerated weathering, the XPS spectra of MPs revealed a peak in the O 1s region, signaling the formation of oxygen-containing functional groups such as hydroxyls, carbonyls, and carboxylates due to photooxidation (Fig. 4a). With increasing weathering duration, here 0, 2 and 10 days, the O 1s peak appears, broadens and increases in intensity, indicating the progressive formation of diverse oxidized moieties on the MP surface. These findings are consistent with prior studies showing that photooxidative aging introduces polar groups that significantly alter surface chemistry and interfacial properties.[17,45,46] Here we investigate how the evolution of the surface chemistry of PE MPs due to environmental weathering would influence the ability of the 12-HSA microtubular foam to retain MPs.

The MP retention efficiency of the microtubular foam remains independent of the weathered state of PE MPs. To evaluate the surface chemistry independence of our microtubular foam-based MP removal method, we tested its performance using MPs subjected to varying degrees of weathering. The 1.5 mg mL^{-1} weathered PE MPs were dispersed in a 10 mg mL^{-1} 12-HSA solution containing ethanolamine at R = 0.5, and the foam was generated following the protocol described earlier, and the MP retention efficiency of foam was quantified using image analysis. Across all weathering stages, we observed no statistically significant change in MP retention efficiency (Fig. 4b). These results confirm that the MP removal process is dominated by physical entrapment within the foam structure rather than by chemical interactions with specific surface functionalities. The microtubule morphology of 12-HSA provides an efficient trap for

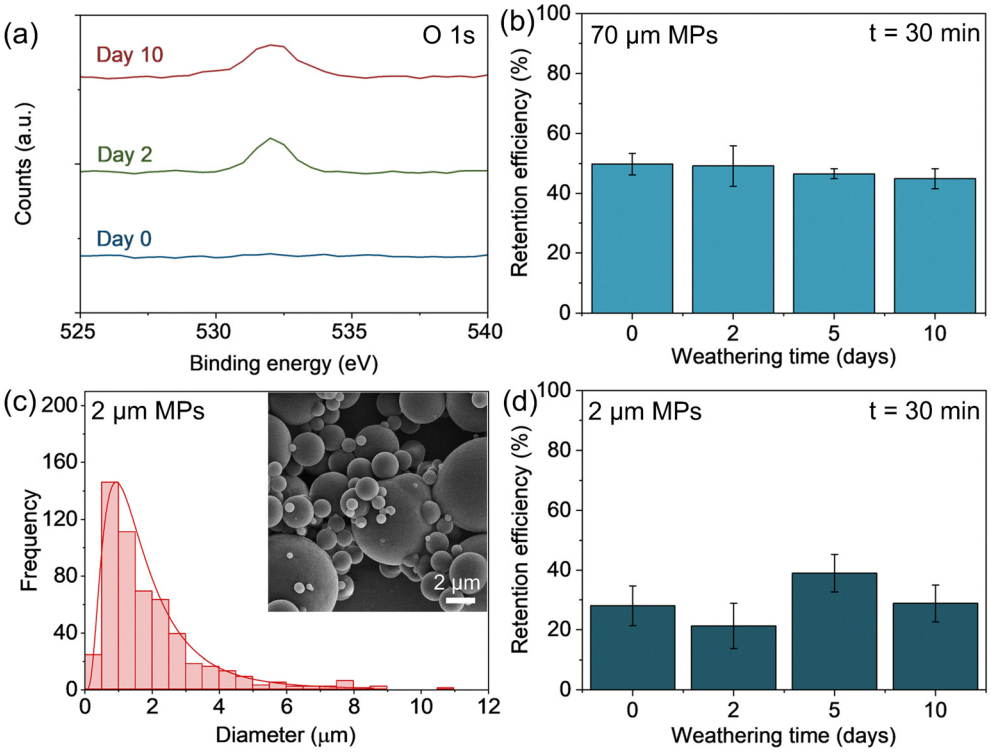

Fig. 4 (a) X-ray photoelectron spectroscopy (XPS) spectra of MPs following different stages of weathering/photooxidation. With increasing weathering time, the O 1s peak appears in the binding energy profile, highlighting the emergence of carbonyl functional groups on the MP surface. (b) Invariance of MP retention efficiency with increasing weathering time for 65 μm MPs. The bars represent the standard error of triplicate measurements. (c) Particle size distribution obtained from image analysis of the smaller PE MPs used in the study. The frequency of the distribution was obtained by analyzing scanning electron microscopy (SEM) images, shown in the inset. The bars represent measured data, the line represents the log-normal distribution fit, and the scale bar in the inset represents 2 μm. (d) MP retention efficiency of microtubular foam for smaller MPs (shown in (c)) with increasing weathering time. The minimal variations in the MP retention efficiency with increasing photooxidation of MPs (weathering time) highlight the primary role of physical forces over chemical interactions in retaining MPs in the microtubular foam phase.

retaining MPs within the thin channels of the foam regardless of particle wettability or oxidation state.

To assess the size-dependence of the MP retention efficiency, we tested the removal of smaller PE MPs of diameter ~2 μm purchased from Cospheric Inc (Fig. 4c). Particles were introduced to the solution of 12-HSA microtubules and subjected to the foaming process described previously. Because of their smaller size, particle retention could not be calculated through bulk imaging as done previously due to the limitations in optically resolving individual MPs. Instead, the retention efficiency was determined by filtration. After allowing the foam to stabilize for 30 minutes, it was separated from the bulk solution and filtered under vacuum to recover any retained particles. Retention efficiency was calculated by comparing the mass of particles recovered on the filter to the initial mass of particles added to the system.

Despite the smaller size and higher diffusivity, a fraction of the smaller MPs were captured and retained within the foam phase of the 12-HSA microtubules (Fig. 4d). Although the MP retention efficiency decreases compared to that observed for larger MPs (Fig. 4b), the microtubular foam remains capable of removing up to 20–40% of smaller MPs in a single cycle. The apparent reduction in the MP removal efficiency upon reducing the MPs size can be attributed to two factors: first, the reduced probability of physical trapping of smaller particles within the foam channels due to their lower inertia and higher mobility (reduced Reynolds number); and second, potential losses during post-processing, particularly during filtration and washing steps. In our protocol, MPs smaller than the pore size of the filter membrane used (pore size ~ 0.7 μm) may pass through and be discarded, leading to underestimation of the actual retention. Further work is needed for precise quantification of the concentration of removed MPs using thermogravimetric, and/or spectroscopic methods. Regardless, the successful removal of a substantial fraction of small MPs demonstrates that the physical entrapment mechanism enabled by the microtubular foam remains operative across a broad MP size range. This robustness further highlights the versatility of our method for MP remediation across a range of sizes.

2.5. Influence of microplastic chemistry

The foam-based method developed here demonstrates the potential to be applied to a wide range of chemically and morphologically diverse MPs. To evaluate the versatility of our approach, we introduced a series of plastics differing in their chemical compositions (Fig. 5). Specifically, we generated chemically diverse MPs from commercially available commodity plastics commonly found in household items. These included polypropylene (PP), polystyrene (PS), polyethylene terephthalate (PET), and polytetrafluoroethylene (PTFE) (Fig. 5a–d). The MPs tested in this study (PP, PE, PS, and PTFE) include several of the most prevalent types detected in marine environments.

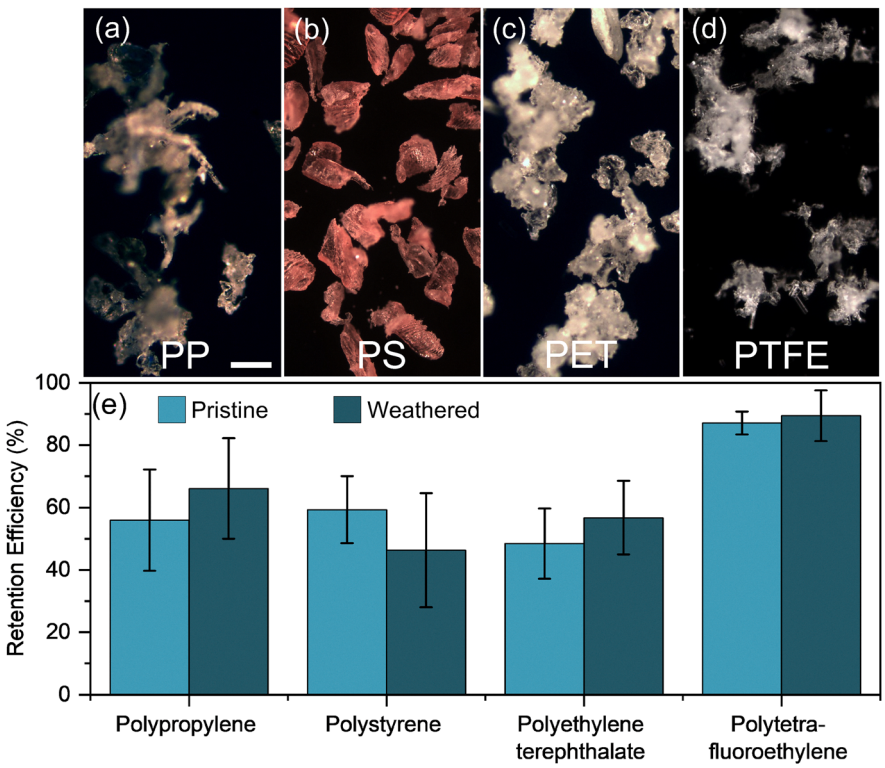

Fig. 5 (a)–(d) Images of MPs produced using physical abrasion of macroplastics of diverse chemistry, specifically (a) PP – polypropylene, (b) PS – polystyrene, (c) PET – polyethylene terephthalate, and (d) PTFE – polytetrafluoroethylene (e) MP retention efficiency of the 12-HSA foam after 30 minutes of equilibration unweathered (light blue) as well as 6-day weathered MPs (dark blue). The error bars in the plot represent the standard deviation of triplicate measurements, indicating that MP retention efficiency is not significantly altered by weathering/photooxidation process.

Meta-analyses have shown that low-density polymers such as PE, PP, and PS dominate polymer types in surface waters due to their high global production volumes and buoyancy characteristics.[47] Thus, the plastic polymers examined in this study are broadly representative of environmentally relevant MPs found in aquatic systems. Although PTFE is less frequently reported in aquatic surveys, it holds environmental relevance as persistent organic pollutant belonging to the broader per- and polyfluoroalkyl substance (PFAS) class.[48] The macroscopic plastics were mechanically abraded into microfragments, which were then collected for analysis. Detailed information on this mechanical transformation process is available in our recent publication.[7] For these experiments, we used a 10 mg mL^{-1} microtubule foam solution with 1.5 mg mL^{-1} of each fragmented MP. The retention efficiency was determined by removing the foam following a 30-minute cycle and quantifying the fragmented plastics that remained in the bulk. Results show that the microtubule foam can effectively remove commodity MPs.

The retention efficiency ranged from 45% to 90% for all plastic types, both in their pristine and six-day weathered states (Fig. 5e). PTFE MPs exhibited slightly higher retention than the other polymers. While PTFE is chemically distinct, the increased retention is more plausibly linked to morphological factors, and the mass density contrast between the MPs and the medium, rather than surface chemistry. Note that 12-HSA is anticipated to spontaneously adsorb onto the MP surfaces, minimizing the influence of the MPs' surface chemistry on retention.[20] Further, PTFE fragments appeared somewhat more anisotropic and dendritic than the other tested MPs (Fig. 5d). The differences in mass density, and anisotropic morphology of PTFE MPs is likely responsible for their enhanced retention. This observation is consistent with the established knowledge that anisotropic particles exhibit greater foam stability due to more effective binding at the fluid–fluid interface, restricting bubble coalescence.[49] However, this interpretation remains qualitative, and further quantitative shape analysis (*e.g.*, fractal dimension or aspect ratio measurements) would be needed to confirm this relationship. These observations highlight the effectiveness of microtubule-based foams in capturing MPs in the foam phase regardless of the MPs' polymeric composition or surface chemistry. This broad applicability is important given that most commercial plastics contain a range of additives that collectively govern their physicochemical properties. Developing MP separation methods that remain effective regardless of the chemical design of the MPs would be especially valuable.

3. Conclusions and outlook

We report a foam-based method for microplastic (MP) removal that relies solely on physical entrapment within a microtubular fatty acid matrix in the foam phase. By leveraging the self-assembly of 12-hydroxystearic acid into microtubules, we generate foams that trap MPs independent of their size, chemistry, or weathered state. The MP retention efficiency of the foam is governed by the anisotropic shape of the self-assembled tubules, which suppress drainage and promote MP capture in the foam phase. The thermoresponsive nature of the tubules enables on-demand foam destabilization and MP release, allowing for straightforward recovery. Repeated foaming cycles further increase the cumulative MP removal, consistent with a probabilistic retention model. Our results show that this method is broadly applicable to a wide range of plastics, including polyethylene, polypropylene, polystyrene, polyethylene terephthalate, and polytetrafluoroethylene, and is effective even after photooxidative aging/weathering. This approach could help in potentially circumventing the limitations of traditional separation techniques that depend on specific surface interactions, providing a generalizable and scalable route for MP removal from aqueous systems.

Despite the conceptual advancements in this study, important questions remain regarding the scalability and practicality of implementing foam-based methods for MP removal in real-world scenarios. The primary focus of this work was to show that MPs can indeed be trapped in the foam phase, both when nanomicelles and microtubules are present, where the MPs remain trapped for longer times in the latter case. However, further research is needed to address several key challenges. These include determining how to selectively retain MPs over other particulate matter commonly found in environmental samples, investigating the applicability of particle and protein-based Pickering foams for MP removal,[20,50] understanding how such a foam-based process could be integrated into existing wastewater treatment plants, and assessing the associated operational costs to ensure commercial viability. At larger scales, foam generation and separation could be achieved using continuous flow systems similar to flotation or froth fractionation units already used in waste treatment. Although a quantitative assessment of energy demands and operational costs was beyond the scope of this study, these parameters will be crucial for evaluating the overall feasibility of implementing such foam-based MP removal processes in real-world applications. Furthermore, it is important to note that the experiments in this study were conducted in model aqueous systems using deionized water. In natural waters, the presence of salts, dissolved organic matter, and colloidal particulates could influence formation and stability by modifying interactions within the fatty acid assemblies. Investigating how these factors affect MP retention represents an important next step toward translating our approach to real-world applications. While answering these questions are beyond the scope of this proof-of-concept demonstration, they represent critical next steps toward developing effective and sustainable solutions to the growing challenge of MP pollution.

Conflicts of interest

There are no conflicts to declare.

Data availability

The data supporting this article have been included as part of the supplementary information (SI). Supplementary information on the size distribution of PE MPs, and details of image analysis to determine retention efficiency of the foam is available. See DOI: **https://doi.org/10.1039/d5sm00850f**.

Acknowledgements

We thank Dr Anne-Laure Fameau (INRAE) for useful discussions. KG was supported by the State of Louisiana and the College of Engineering at LSU through a Flagship Assistantship. Authors thank Anding Professorship at LSU for financial support. A portion of this research was performed at the Spallation Neutron Source, a DOE Office of Science User Facility operated by Oak Ridge National Laboratory. We acknowledge Dr Jong Keum for small-angle X-ray scattering (SAXS) data measurement on the Xeuss 3.0 SAXS instrument *via* the Oak Ridge National Laboratory (ORNL) instrumentation pool. Dr Jong Keum is supported by both Center for Nanophase Materials Sciences (CNMS) and Neutron Scattering Division (NSD), which are U.S. Department of Energy, Office of Science User Facilities.

References

1 M. MacLeod, H. P. H. Arp, M. B. Tekman and A. Jahnke, The global threat from plastic pollution, *Science*, 2021, **373**(6550), 61–65.
2 N. B. Hartmann, T. Hüffer, R. C. Thompson, M. Hassellöv, A. Verschoor, A. E. Daugaard, S. Rist, T. Karlsson, N. Brennholt, M. Cole, M. P. Herrling, M. C. Hess, N. P. Ivleva, A. L. Lusher and M. Wagner, Are We Speaking the Same Language? Recommendations for a Definition and Categorization Framework for Plastic Debris, *Environ. Sci. Technol.*, 2019, **53**(3), 1039–1047.
3 S. Abbasi, A. Turner, M. Hoseini and H. Amiri, Microplastics in the Lut and Kavir Deserts, Iran, *Environ. Sci. Technol.*, 2021, **55**(9), 5993–6000.
4 S. Allen, D. Allen, V. R. Phoenix, G. Le Roux, P. Durántez Jiménez, A. Simonneau, S. Binet and D. Galop, Atmospheric transport and deposition of microplastics in a remote mountain catchment, *Nat. Geosci.*, 2019, **12**(5), 339–344.
5 C. L. Waller, H. J. Griffiths, C. M. Waluda, S. E. Thorpe, I. Loaiza, B. Moreno, C. O. Pacherres and K. A. Hughes, Microplastics in the Antarctic marine system: An emerging area of research, *Sci. Total Environ.*, 2017, **598**, 220–227.
6 A. Al Harraq and B. Bharti, Microplastics through the Lens of Colloid Science, *ACS Environ. Au*, 2022, **2**(1), 3–10.
7 P. J. Brahana, A. Al Harraq, L. E. Saab, R. Roberg, K. T. Valsaraj and B. Bharti, Uptake and release of perfluoroalkyl carboxylic acids (PFCAs) from macro and microplastics, *Environ. Sci.: Processes Impacts*, 2023, **25**(9), 1519–1531.
8 I. Velzeboer, C. J. A. F. Kwadijk and A. A. Koelmans, Strong Sorption of PCBs to Nanoplastics, Microplastics, Carbon Nanotubes, and Fullerenes, *Environ. Sci. Technol.*, 2014, **48**(9), 4869–4876.
9 S. H. Joo, Y. Liang, M. Kim, J. Byun and H. Choi, Microplastics with adsorbed contaminants: Mechanisms and Treatment, *Environ. Challenges*, 2021, **3**, 100042.
10 N. B. Hartmann, S. Rist, J. Bodin, L. H. Jensen, S. N. Schmidt, P. Mayer, A. Meibom and A. Baun, Microplastics as vectors for environmental contaminants: Exploring sorption, desorption, and transfer to biota, *Integr. Environ. Assess. Manage.*, 2017, **13**(3), 488–493.
11 P. Brahana, M. Zhang, E. Nakouzi and B. Bharti, Weathering influences the ice nucleation activity of microplastics, *Nat. Commun.*, 2024, **15**(1), 9579.
12 A. Al Harraq, P. J. Brahana and B. Bharti, Colloid and Interface Science for Understanding Microplastics and Developing Remediation Strategies, *Langmuir*, 2025, **41**(7), 4412–4421.
13 M. Shen, B. Song, Y. Zhu, G. Zeng, Y. Zhang, Y. Yang, X. Wen, M. Chen and H. Yi, Removal of microplastics *via* drinking water treatment: Current knowledge and future directions, *Chemosphere*, 2020, **251**, 126612.
14 M. Lapointe, J. M. Farner, L. M. Hernandez and N. Tufenkji, Understanding and Improving Microplastic Removal during Water Treatment: Impact of Coagulation and Flocculation, *Environ. Sci. Technol.*, 2020, **54**(14), 8719–8727.
15 Y. Zhang, H. Jiang, K. Bian, H. Wang and C. Wang, Is froth flotation a potential scheme for microplastics removal? Analysis on flotation kinetics and surface characteristics, *Sci. Total Environ.*, 2021, **792**, 148345.
16 T. F. Mendes, A. S. Reis, A. C. Silva and M. A. S. Barrozo, Analysis of the Effect of Surfactants on the Performance of Apatite Column Flotation, *Minerals*, 2024, **14**(8), 840.
17 A. Al Harraq, P. J. Brahana, O. Arcemont, D. Zhang, K. T. Valsaraj and B. Bharti, Effects of Weathering on Microplastic Dispersibility and Pollutant Uptake Capacity, *ACS Environ. Au*, 2022, **2**(6), 549–555.
18 C. D. Rummel, O. J. Lechtenfeld, R. Kallies, A. Benke, P. Herzsprung, R. Rynek, S. Wagner, A. Potthoff, A. Jahnke and M. Schmitt-Jansen, Conditioning Film and Early Biofilm Succession on Plastic Surfaces, *Environ. Sci. Technol.*, 2021, **55**(16), 11006–11018.
19 A. J. Pete, P. J. Brahana, M. Bello, M. G. Benton and B. Bharti, Biofilm Formation Influences the Wettability and Settling of Microplastics, *Environ. Sci. Technol. Lett.*, 2022, **10**(2), 159–164.
20 Y. Ma, Y. Wu, J. G. Lee, L. He, G. Rother, A.-L. Fameau, W. A. Shelton and B. Bharti, Adsorption of Fatty Acid Molecules on Amine-Functionalized Silica Nanoparticles: Surface Organization and Foam Stability, *Langmuir*, 2020, **36**(14), 3703–3712.
21 A.-L. Fameau, A. Arnould and A. Saint-Jalmes, Responsive self-assemblies based on fatty acids, *Curr. Opin. Colloid Interface Sci.*, 2014, **19**(5), 471–479.
22 I. Johansson and M. Svensson, Surfactants based on fatty acids and other natural hydrophobes, *Curr. Opin. Colloid Interface Sci.*, 2001, **6**(2), 178–188.

23 J.-P. Douliez, C. Gaillard, L. Navailles and F. Nallet, Novel Lipid System Forming Hollow Microtubes at High Yields and Concentration, *Langmuir*, 2006, **22**(7), 2942–2945.
24 A. Saint-Jalmes, Physical chemistry in foam drainage and coarsening, *Soft Matter*, 2006, **2**(10), 836–849.
25 B. Bharti, A.-L. Fameau, M. Rubinstein and O. D. Velev, Nanocapillarity-mediated magnetic assembly of nanoparticles into ultraflexible filaments and reconfigurable networks, *Nat. Mater.*, 2015, **14**(11), 1104–1109.
26 Z. Gricius and G. Øye, Recent advances in the design and use of Pickering emulsions for wastewater treatment applications, *Soft Matter*, 2023, **19**(5), 818–840.
27 H. Yu, Y. Zhu, A. Hui, F. Yang and A. Wang, Removal of antibiotics from aqueous solution by using porous adsorbent templated from eco-friendly Pickering aqueous foams, *J. Environ. Sci.*, 2021, **102**, 352–362.
28 A.-L. Fameau and M. A. Rogers, The curious case of 12-hydroxystearic acid—the Dr Jekyll & Mr Hyde of molecular gelators, *Curr. Opin. Colloid Interface Sci.*, 2020, **45**, 68–82.
29 M. Almeida, D. Dudzinski, C. Amiel, J.-M. Guigner, S. Prévost, C. Le Coeur and F. Cousin, Aqueous Binary Mixtures of Stearic Acid and Its Hydroxylated Counterpart 12-Hydroxystearic Acid: Cascade of Morphological Transitions at Room Temperature, *Molecules*, 2023, **28**(11), 4336.
30 A.-L. Fameau and T. Zemb, Self-assembly of fatty acids in the presence of amines and cationic components, *Adv. Colloid Interface Sci.*, 2014, **207**, 43–64.
31 A.-L. Fameau, F. Cousin and A. Saint-Jalmes, Morphological Transition in Fatty Acid Self-Assemblies: A Process Driven by the Interplay between the Chain-Melting and Surface-Melting Process of the Hydrogen Bonds, *Langmuir*, 2017, **33**(45), 12943–12951.
32 J. V. Selinger, M. S. Spector and J. M. Schnur, Theory of Self-Assembled Tubules and Helical Ribbons, *J. Phys. Chem. B*, 2001, **105**(30), 7157–7169.
33 A.-L. Fameau and S. Fujii, Stimuli-responsive liquid foams: From design to applications, *Curr. Opin. Colloid Interface Sci.*, 2020, **50**, 101380.
34 A.-L. Fameau, A. Saint-Jalmes, F. Cousin, B. Houinsou Houssou, B. Novales, L. Navailles, F. Nallet, C. Gaillard, F. Boué and J.-P. Douliez, Smart Foams: Switching Reversibly between Ultrastable and Unstable Foams, *Angew. Chem., Int. Ed.*, 2011, **50**(36), 8264–8269.
35 G. Erni-Cassola, V. Zadjelovic, M. I. Gibson and J. A. Christie-Oleza, Distribution of plastic polymer types in the marine environment; A meta-analysis, *J. Hazard. Mater.*, 2019, **369**, 691–698.
36 C. A. Schneider, W. S. Rasband and K. W. Eliceiri, NIH Image to ImageJ: 25 years of image analysis, *Nat. Methods*, 2012, **9**(7), 671–675.
37 A.-L. Fameau, F. Cousin, L. Navailles, F. Nallet, F. Boué and J.-P. Douliez, Multiscale Structural Characterizations of Fatty Acid Multilayered Tubes with a Temperature-Tunable Diameter, *J. Phys. Chem. B*, 2011, **115**(29), 9033–9039.
38 J.-P. Douliez, B. Pontoire and C. Gaillard, Lipid Tubes with a Temperature-Tunable Diameter, *ChemPhysChem*, 2006, **7**(10), 2071–2073.
39 M. Pivokonsky, L. Cermakova, K. Novotna, P. Peer, T. Cajthaml and V. Janda, Occurrence of microplastics in raw and treated drinking water, *Sci. Total Environ.*, 2018, **643**, 1644–1651.
40 Z. Wang, T. Lin and W. Chen, Occurrence and removal of microplastics in an advanced drinking water treatment plant (ADWTP), *Sci. Total Environ.*, 2020, **700**, 134520.
41 W. Perren, A. Wojtasik and Q. Cai, Removal of Microbeads from Wastewater Using Electrocoagulation, *ACS Omega*, 2018, **3**(3), 3357–3364.
42 B. Gewert, M. M. Plassmann and M. MacLeod, Pathways for degradation of plastic polymers floating in the marine environment, *Environ. Sci.: Processes Impacts*, 2015, **17**(9), 1513–1521.
43 A. L. Andrady, Microplastics in the marine environment, *Mar. Pollut. Bull.*, 2011, **62**(8), 1596–1605.
44 A. International, *ASTM D5071-06 Standard Practice for Exposure of Photodegradable Plastics in Xenon Arc Apparatus*, 2021.
45 J. Brandon, M. Goldstein and M. D. Ohman, Long-term aging and degradation of microplastic particles: Comparing in situ oceanic and experimental weathering patterns, *Mar. Pollut. Bull.*, 2016, **110**(1), 299–308.
46 P. Liu, X. Zhan, X. Wu, J. Li, H. Wang and S. Gao, Effect of weathering on environmental behavior of microplastics: Properties, sorption and potential risks, *Chemosphere*, 2020, **242**, 125193.
47 G. Erni-Cassola, V. Zadjelovic, M. I. Gibson and J. A. Christie-Oleza, Distribution of plastic polymer types in the marine environment; A meta-analysis, *J. Hazard. Mater.*, 2019, **369**, 691–698.
48 B. J. Henry and N. Timmer, Environmental fate and behavior studies of a polymeric PFAS, polytetrafluoroethylene (PTFE) – results and application to risk assessment, *Chemosphere*, 2025, **385**, 144569.
49 P. Amani, R. Miller, A. Javadi and M. Firouzi, Pickering foams and parameters influencing their characteristics, *Adv. Colloid Interface Sci.*, 2022, **301**, 102606.
50 L. Hassan, C. Xu, M. Boehm, S. K. Baier and V. Sharma, Ultrathin Micellar Foam Films of Sodium Caseinate Protein Solutions, *Langmuir*, 2023, **39**(17), 6102–6112.

